Inorg. Chem. **2008**, *47*, 11711−11719

Dinuclear Zinc Complexes Using Pentadentate Phenolate Ligands

Paul D. Knight, Andrew J. P. White, and Charlotte K. Williams*

Department of Chemistry, Imperial College London, London, SW7 2AZ, U.K.

Received July 29, 2008

The synthesis and characterization of 15 dinuclear zinc complexes are reported, including the X-ray crystal structures of 5 complexes. The ligand motif utilizing *p*-cresol as a bridging unit between the two zinc centers and a set of three related ligands has been synthesized; 2,6-*bis*(R)-*p*-cresol (where R is $CH_2NMe(CH_2)_2NMe_2$ = L^1, $CH{=}N(CH_2)_2NMe_2$ = L^2, and $CH_2NH(CH_2)_2NMe_2$ = L^3). Dizinc trihalide complexes [$L^nZn_2(\mu$-X)X_2] (where X = Cl, Br, I) have been prepared. The trihalide complexes were treated with potassium ethoxide, resulting in quantitative substitution of the bridging halide group to give [$L^nZn_2(\mu$-OEt)X_2]. The dizinc ethoxide complexes were tested in situ as initiators for lactide ring opening polymerization. Dizinc triacetate complexes have also been synthesized [$L^nZn_2(OAc)_3$], as well as cationic diacetate species containing two bridging acetate groups, [$L^nZn_2(\mu$-OAc)$_2$][BPh_4]. Structural differences between complexes of the three ligands are discussed.

Introduction

Over the past few decades, there has been much research into bimetallic complexes due to the interesting properties arising from the close proximity of the two metal centers.[1] These include studies of bimetallic complexes' magnetic, electronic, spectroscopic, and structural properties, as well as their reactivity.[1,2] Binuclear zinc complexes have attracted particular interest as important structural mimics of the active site of a range of metalloenzymes,[3] such as zinc-dependent aminopeptidases, metallo-β-lactamases, and alkaline phosphatases.[4] In addition, these synthetic dizinc complexes have allowed new catalytic processes to be developed that are beyond the scope of natural enzymes. These processes include Mannich-type reactions,[5] Aldol reactions,[6] Friedel−Crafts alkylations,[7] alkynylation reactions,[8] as well as polymerization catalysis.[9]

* c.k.williams@imperial.ac.uk.

(1) Gavrilova, A. L; Bosnich, B. *Chem. Rev.* **2004**, *104*, 349.

(2) (a) Paulucci, G.; Vigato, P. A.; Rossetto, G.; Casellato, U. *Inorg. Chim. Acta* **1982**, L71. (b) Xiaoxeng, L.; Genglin, W.; Daizheng, L.; Shiping, Y.; Zonghui, J. *Polyhedron* **1995**, *14*, 511. (c) Cheng, P.; Liao, D.; Yan, S.; Jiang, S.; Wang, G. *Polyhedron* **1995**, *14*, 2355. (d) Mikuriya, M.; Tashima, S. *Polyhedron* **1998**, *17*, 207. (e) Erxleben, A. *Inorg. Chem.* **2001**, *40*, 208. (f) Adams, H.; Bradshaw, D.; Fenton, D. E. *Polyhedron* **2002**, *21*, 1957. (g) Adams, H.; Bradshaw, D.; Fenton, D. E. *Inorg. Chim. Acta* **2002**, *332*, 195. (h) Ye, B.-H.; Li, X.-Y.; Williams, I. D.; Chen, X.-M. *Inorg. Chem.* **2002**, *41*, 6426. (i) Adams, H.; Cummings, L. R.; Fenton, D. E.; McHugh, P. E. *Inorg. Chem. Commun.* **2003**, *6*, 19. (j) Dutta, B.; Bag, P.; Flörke, U.; Nag, K. *Inorg. Chem.* **2005**, *44*, 147. (k) Shanmuga Bharathi, K.; Kalilur Rahiman, A.; Rajesh, K.; Sreedaran, S.; Aravindan, P. G.; Velmurugan, D.; Narayanan, V. *Polyhedron* **2006**, *25*, 2859. (l) Biswas, P.; Ghosh, M.; Dutta, S. K.; Flörke, U.; Nag, K. *Inorg. Chem.* **2006**, *45*, 4830. (m) Ambrosi, G.; Formica, M.; Fusi, V.; Giorgi, L.; Guerri, A.; Micheloni, M.; Paoli, P.; Pontellini, R.; Rossi, P. *Inorg. Chem.* **2007**, *46*, 309. (n) Doyle, D. J.; Gibson, V. C.; White, A. J. P. *Dalton Trans.* **2007**, 358.

(3) (a) Parkin, G. *Chem. Rev.* **2004**, *104*, 699. (b) Vahrenkamp, H. *Dalton Trans.* **2007**, 4751.

(4) (a) Yamami, M.; Tanaka, M.; Sakiyama, H.; Koga, T.; Kobayashi, K.; Miyasaka, H.; Ohba, M.; Okawa, H. *Dalton Trans.* **1997**, 4545. (b) Sakiyama, H.; Mochizuki, R.; Sugawara, A.; Sakamoto, M.; Nishida, Y.; Yamasaki, M. *Dalton Trans.* **1999**, 997. (c) Kaminskaia, N. V.; Spingler, B.; Lippard, S. J. *J. Am. Chem. Soc.* **2000**, *122*, 6411. (d) Erxleben, A.; Hermann, J. *Dalton Trans.* **2000**, 569. (e) Abe, K.-J.; Izumi, J.; Ohba, M.; Yokoyama, T.; Okawa, H. *Bull. Chem. Soc. Jpn.* **2001**, *74*, 85. (f) Sakiyama, H.; Igarashi, Y.; Nakayama; Hossain, M. J.; Unoura, K.; Nishida, Y. *Inorg. Chim. Acta* **2003**, *351*, 256. (g) Chen, J.; Wang, X.; Zhu, Y.; Lin, J.; Yang, X.; Li, Y.; Lu, Y.; Guo, Z. *Inorg. Chem.* **2005**, *44*, 3424. (h) Jikido, R.; Shiraishi, H.; Matsufuji, K.; Ohba, M.; Furutachi, H.; Suzuki, M.; Okawa, H *Bull. Chem. Soc. Jpn.* **2005**, *78*, 1795. (i) Sakiyama, H.; Ono, K.; Suzuki, T.; Tone, K.; Ueno, T.; Nishida, Y. *Inorg. Chem. Commun.* **2005**, *8*, 372. (j) Tamilselvi, A; Nethaji, M.; Mugesh, G. *Chem. Eur. J.* **2006**, *12*, 7797. (k) Mitiæ, N.; Smith, S. J.; Neves, A.; Guddat, L. W.; Gahan, L. R.; Schenk, G. *Chem. Rev.* **2006**, *106*, 3338.

(5) (a) Trost, B. M.; Jaratjaroonphong, J.; Reutrakul, V. *J. Am. Chem. Soc.* **2006**, *128*, 2778. (b) Trost, B. M.; Lupton, D. W. *Org. Lett.* **2007**, *9*, 2023.

(6) Trost, B. M.; Shin, S.; Sclafini, J. A. *J. Am. Chem. Soc.* **2005**, *127*, 8602.

(7) Trost, B. M.; Müller, C. *J. Am. Chem. Soc.* **2008**, *130*, 2438.

(8) Trost, B. M.; Weiss, A. H.; von Wangelin, A. J. *J. Am. Chem. Soc.* **2006**, *128*, 8.

(9) (a) Williams, C. K.; Brooks, N. R.; Hillmyer, M. A.; Tolman, W. B. *Chem. Commun.* **2002**, 2132. (b) Breyfogle, L. E.; Williams, C. K., Jr.; Hillmyer, M. A.; Tolman, W. B. *Dalton Trans.* **2006**, 928. (c) Garner, L. E.; Zhu, H.; Hlavinka, M. L.; Hagadorn, J. R.; Chen, E. Y.-X. *J. Am. Chem. Soc.* **2006**, *128*, 14822. (d) Champouret, Y. D. M.; Nodes, W. J.; Scrimshire, J. A.; Singh, K.; Solan, G. A.; Young, I. *Dalton Trans.* **2007**, 4565.

10.1021/ic8014173 CCC: $40.75
Published on Web 11/18/2008

Scheme 1. Structures of HL^{1-3} and synthesis of the dizinc complexes

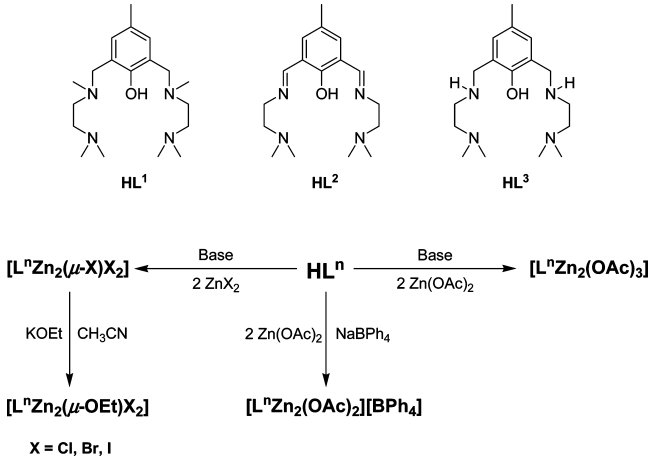

A common motif in the design of dinucleating ligands involves an alkoxide or phenoxide group that bridges the two metal centers, and the remainder of the ligand construct usually requires further coordinating groups to retain the metal atoms and prevent formation of multinuclear arrays. Some examples of this type of ligand are shown in Scheme 1, and the zinc complexes derived from L^{1-3} will be the focus of this study. Dinuclear zinc complexes of these ligands[4d,e,h] and related systems[2g,h,k,4b,f,i,9d,10] have been studied previously to generate cationic acetate complexes of the type $[LZn_2(\mu\text{-}OAc)_2]^+$. Some neutral complexes, for example using nitrate or isothiocyanate coligands, have also been studied;[2i,4c] and in general the syntheses are undertaken in aqueous environments. Although these complexes have been tested in biologically relevant reactions (vide supra), we were interested in studying anhydrous, neutral species for lactide ring opening polymerization and CO_2/epoxide copolymerization catalysis, which have both been demonstrated previously with zinc-based systems.[9a,b,11,12] For such catalysis, an alkoxide or carboxylate coligand is generally required for the initiation step. Examples of monomeric dizinc alkoxide complexes are rare,[4c,13] but one such complex based on HL^1 and synthesized by Williams et al.,[9a,b] has been shown to have high catalytic reactivity in lactide ring-opening polymerization. However, the synthetic route to the reported complex, $[L^1Zn_2(\mu\text{-}OEt)Cl_2]$, was rather complex and of limited generality. An important goal of this study was to develop simpler and more efficient routes to dinuclear zinc alkoxide complexes by utilizing potassium alkoxide metathesis reactions[14] with the corresponding dizinc trihalide complexes $[[L^nZn_2(\mu\text{-}X)X_2]$. The dizinc alkoxide complexes were applied as initiators in the ring opening polymerization of lactide. In addition, the neutral acetate complexes, $[L^nZn_2(OAc)_3]$, were targeted for catalytic testing in CO_2/epoxide copolymerizations, as well as being model compounds to probe structural features of the complexes.

Results and Discussion

The preligands HL^{1-3} (Scheme 1) were prepared in high yield by modifications of literature procedures (see Supporting Information for details).[4d,15]

$[L^1Zn_2(\mu\text{-}X)X_2]$. The synthesis of the dizinc trihalide complexes (i.e., $[LZn_2(\mu\text{-}X)X_2]$, where X = Cl, Br, I) was achieved in three ways; simply by mixing the preligand and the zinc halide species in an appropriate solvent; by adding a base to this mixture; or by preforming the ligand alkali salt, followed by a salt elimination reaction with the zinc halide. All the methods were successful, but the metathesis reaction generally led to better yields of high-purity material. The syntheses of $[L^1Zn_2(\mu\text{-}Cl)Cl_2]$ and $[L^1Zn_2(\mu\text{-}Br)Br_2]$ yielded white solids that had low solubility in methanol or THF. The ^1H NMR spectrum of $[L^1Zn_2(\mu\text{-}Cl)Cl_2]$, in $CDCl_3$, shows a single aromatic peak at 6.75 ppm. The terminal NMe_2 groups are also observed as a single peak, as are the internal NMe groups at 2.61 ppm and 2.16 ppm, respectively. However, the aromatic CH_2 protons resonate as a pair of AB doublets at 4.36 and 3.11 ppm; indicating that the complex is chiral. The remaining CH_2 protons in the ethylene diamine units are also diastereotopic and are observed as two pairs of multiplets between 2.86 and 3.00 ppm and 2.45 and 2.56 ppm. The ^1H NMR spectrum of the bromide complex is very similar, and both complexes are symmetrical on the NMR time scale, at 298 K. Using a similar method to synthesize $[L^1Zn_2(\mu\text{-}I)I_2]$ failed to yield a precipitate from methanol or THF, and only an off-white/yellow material could be obtained upon solvent removal. Recrystallization

(10) (a) Asato, E.; Chinen, M.; Yoshitno, A.; Sakata, Y; Sigiura, K.-I. *Chem. Lett.* **2000**, 678. (b) Fenton, D. E. *Inorg. Chem. Commun.* **2002**, *5*, 537.

(11) (a) Sugimoto, H.; Inoue, S. *J. Polym. Sci. Part A: Polym. Chem.* **2004**, *42*, 5561. (b) Coates, G. W.; Moore, D. R. *Angew. Chem., Int. Ed.* **2004**, *43*, 6618. (c) Schenk, S.; Notni, J.; Köhn, U.; Wermann, K.; ers, E. *Dalton Trans.* **2006**, 4191. (d) Darensbourg, D. J.; Lewis, S. J.; Rodgers, J. L.; Yarbrough, J. C. *Inorg. Chem.* **2003**, *42*, 581. (e) van Meerendonk, W. J.; Duchateau, R.; Koning, C. E.; Gruter, G.-J. M. *Macromolecuels* **2005**, *38*, 7306. (f) Bok, T.; Yun, H.; Lee, B. Y. *Inorg. Chem.* **2006**, *45*, 4228. (g) Xiao, Y.; Wang, Z.; Ding, K. *Macromolecules* **2006**, *39*, 2006. (h) Liu, B.; Tian, C.; Zhang, L.; Yan, W.; Zhang, W. *J. Polym. Sci. Part A: Polym. Chem.* **2006**, *44*, 6243. (j) Pilz, M. F.; Limberg, C.; Lazarov, B. B.; Hultzsch, K. C.; Ziemer, B. *Organometallics* **2007**, *26*, 3668. (i) Sugimoto, H.; Ogawa, A. *React. Funct. Polym.* **2007**, *67*, 1277.

(12) (a) Dechy-Cabaret, O.; Martin-Vaca, B.; Bourissou, D. *Chem. Rev.* **2004**, *104*, 6147. (b) Platel, R. H.; Hodgson, L. M.; Williams, C. K. *Polym. Rev.* **2008**, *48*, 11. (c) Cheng, M.; Attygale, A. B.; Lobkovsky, E. B.; Coates, G. W. *J. Am. Chem. Soc.* **1999**, *121*, 11583. (d) Chamberlain, B. M.; Cheng, M.; Moore, D. R.; Ovitt, T. M.; Lobkovsky, E. B.; Coates, G. W. *J. Am. Chem. Soc.* **2001**, *123*, 3229. (e) Chisholm, M. H.; Eilerts, N. W.; Huffman, J. C.; Iyer, S. S.; Pacold, M.; Phomphrai, K. *J. Am. Chem. Soc.* **2000**, *122*, 11845. (f) Chisholm, M. H.; Huffman, J. C.; Phomphrai, K. *J. Chem. Soc., Dalton Trans.* **2001**, 222. (g) Chisholm, M. H.; Gallucci, J. C.; Zhen, H. H.; Huffman, J. C. *Inorg. Chem.* **2001**, *40*, 5051. (h) Chisholm, M. H.; Gallucci, J.; Phomphrai, K. *Inorg. Chem.* **2002**, *41*, 2785. (i) Williams, C. K.; Breyfogle, L. E.; Choi, S. K.; Nam, W. W., Jr.; Hillmyer, M. A.; Tolman, W. B. *J. Am. Chem. Soc.* **2003**, *123*, 11350. (j) Chen, H. Y.; Tang, H. Y.; Lin, C. C. *Macromolecules* **2006**, *39*, 3745. (k) Huang, B. H.; Lin, C. N.; Hsueh, M. L.; Athar, T.; Lin, C. C. *Polymer* **2006**, *47*, 6622. (l) Lian, B.; Thomas, C. M., Jr.; Lehmann, C. W.; Roisnel, T.; Carpentier, J. F. *Inorg. Chem.* **2007**, *46*, 328.

(13) (a) Drago, R. S.; Desmond, M. J.; Cordon, B. B.; Miller, K. A. *J. Am. Chem. Soc.* **1983**, *105*, 2287. (b) Fondon, M; Garcia-Deibe, A. M.; Ocampo, N.; Sanmartin, J.; Bermejo, M. R. *Dalton Trans.* **2004**, 2135. (c) Hlavinka, M. L.; McNevin, M. J.; Shoemaker, R.; Hagadorn, J. R. *Inorg. Chem.* **2006**, *45*, 1815.

(14) Cheng, M.; Moore, D. R.; Reczek, J. J.; Chamberlain, B. M.; Lobkovsky, E. B.; Coates, G. W. *J. Am. Chem. Soc.* **2001**, *123*, 8738.

(15) Higuchi, C.; Sakiyama, H.; Okawa, H.; Fenton, D. E. *Dalton Trans.* **1995**, 4015.

of the crude material yielded a microcrystalline solid. However, the ^{1}H NMR spectrum shows multiple broadened peaks and indicates more than one species is present in solution. The aromatic region contains one major and at least two minor peaks, all of differing integrations. Three major peaks are observed for the NMe_2, NMe, and ArMe groups, which are slightly broadened, but several smaller peaks are also observed in similar regions, and at least two pairs of doublets are assigned to the CH_2 protons. Nevertheless, elemental analysis was in agreement with the formula $[L^1Zn_2I_3]$, and the FAB mass spectrum shows a group of peaks at 721 amu, assigned to $[M-I]^+$ (and is consistent with the FAB mass spectrum of the chloride and bromide complexes). The ^{1}H NMR spectrum of $[L^1Zn_2(\mu\text{-}I)I_2]$ is rationalized by different structural isomers of the complex; the two coordinated NMe groups can adopt different conformations (i.e., *RR*, *SS*, *RS*, and *SR*); the five-membered chelate rings may also adopt different conformations, and further possible isomers may arise from the coordination modes around the zinc centers. These conformations are usually expected to rapidly interconvert, but may be slowed in the iodide complex due to the increased size of the iodide groups compared with chloride and bromide. VT ^{1}H NMR spectroscopy (d_2-TCE) showed convergence at 368 K, and averaged broadened resonances were observed.

$[L^1Zn_2(\mu\text{-}OEt)X_2]$. Following the successful syntheses of the dizinc trihalide complexes, the alkoxide species $[L^1Zn_2(\mu\text{-}OEt)X_2]$ were prepared in quantitative yield by a salt metathesis reaction between the bridging halide group and potassium ethoxide.[14] The reactions were carried out under nitrogen, in Youngs tap NMR tubes using CD_3CN as solvent, and were monitored by ^{1}H NMR spectroscopy. In the case of $[L^1Zn_2(\mu\text{-}Cl)Cl_2]$, a reaction was observed within 30 min to generate a mixture of new species that had significant broadening of all the peaks in the ^{1}H NMR spectrum. Upon comparing the integration of the aromatic protons with the CH_2, NMe, and ArMe integrals, as well as those of the new ethoxide groups (at ca. 1.19 ppm and 3.92 ppm), we proposed the formation of the desired species $[L^1Zn_2(\mu\text{-}OEt)Cl_2]$. This was confirmed by removal of the solvent and addition of CD_2Cl_2, the resulting ^{1}H NMR spectrum was in agreement with the structure previously reported.[9a] The reactions of $[L^1Zn_2(\mu\text{-}Br)Br_2]$ and $[L^1Zn_2(\mu\text{-}I)I_2]$ with potassium ethoxide in CD_3CN proceeded in a similar manner to that of $[L^1Zn_2(\mu\text{-}Cl)Cl_2]$. After 30 min, several new species were present in the NMR spectra and showed similar features to the spectrum of $[L^1Zn_2(\mu\text{-}OEt)Cl_2]$. Upon leaving the NMR tube reaction of $[L^1Zn_2(\mu\text{-}I)I_2]$ and KOEt, crystals of $[L^1Zn_2(\mu\text{-}OEt)I_2]$ were obtained.

X-ray Crystallography. The molecular structure of $[L^1Zn_2(\mu\text{-}OEt)I_2]$ is shown in Figure 1. With the exception of the ethoxide bridging unit (based on O(30)), the complex shows approximate C_2 symmetry about an axis coincident with the C(1)—O(1) vector. The two *N*,*N*′ five-membered chelate rings have the same configuration (both λ in Figure 1). (The complex crystallized in a racemic space group, so the crystal contains equal numbers of the molecule shown in Figure 1 and its enantiomer).

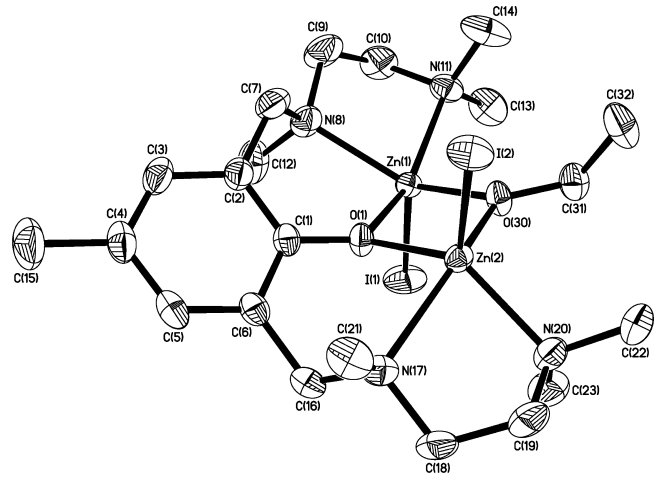

Figure 1. The molecular structure of $[L^1Zn_2(\mu\text{-}OEt)I_2]$ (50% probability ellipsoids).

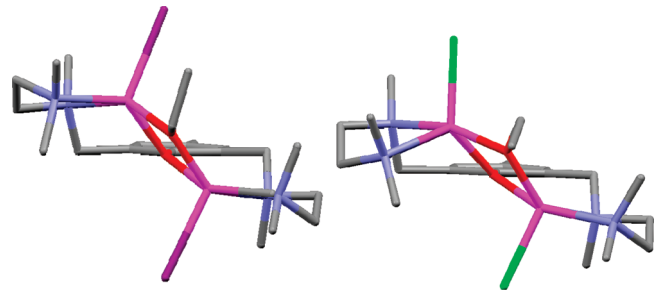

Figure 2. Projection of the molecular structure of $[L^1Zn_2(\mu\text{-}OEt)I_2]$ (left) and $[L^1Zn_2(\mu\text{-}OEt)Cl_2]$[9a] (right) along the phenolate axis.

Table 1. Selected Bond Lengths (Å) and Angles (°) for $[L^1Zn_2(\mu\text{-}OEt)I_2]$

Zn(1)—N(8)	2.194(2)	Zn(2)—N(17)	2.396(2)
Zn(1)—O(1)	2.0885(17)	Zn(2)—O(1)	2.0008(17)
Zn(1)—O(30)	1.9758(17)	Zn(2)—O(30)	2.0375(18)
Zn(1)···Zn(2)	3.1700(6)	O(1)—C(1)	1.344(3)
Zn(1)—O(1)—Zn(2)	101.62(7)	Zn(1)—O(30)—Zn(2)	104.34(8)

Table 2. Selected Bond Lengths (Å) and Angles (°) for the Two Independent Complexes ($[L^2Zn_2(\mu\text{-}I)I_2]$-**I** and $[L^2Zn_2(\mu\text{-}I)I_2]$-**II**) Present in the Crystals of $[L^2Zn_2(\mu\text{-}I)I_2]$

	isomer **I**	isomer **II**
Zn(1)—O(1)	2.033(2)	2.071(3)
Zn(2)—I(3)	2.6951(5)	2.6841(5)
Zn(2)—N(14)	2.064(3)	2.059(3)
Zn(1)···Zn(2)	3.4248(5)	3.4591(6)
Zn(1)—I(3)	2.8006(5)	2.7221(5)
Zn(1)—N(7)	2.086(3)	2.074(4)
Zn(2)—O(1)	2.141(3)	2.130(3)
O(1)—C(1)	1.319(4)	1.320(4)
Zn(1)—I(3)—Zn(2)	77.070(13)	79.556(15)
Zn(1)—O(1)—Zn(2)	110.24(12)	110.86(12)

When viewed along the phenolate bond (Figure 2), the C(7)—N(8) and C(16)—N(17) bonds of the pendant arms of the molecule are essentially perpendicular to the plane of the aromatic ring, giving the molecule a distinct chirality. The zinc centers are both five coordinate with distorted square pyramidal geometries. The bond distances (Table 1) between the phenolate oxygen atom (O(1)) and the two zinc centers are somewhat different, with a shorter phenolate bond (2.0008(17) Å) to Zn(2). The bond distances between the ethoxide oxygen (O(30)) and the two zinc centers are also different, with a shorter ethoxide bond (1.9758(17) Å) to

Zn(1). The distance between the two zinc atoms is 3.1700(6) Å, and both coordinated NMe groups (N(8) and N(17)) have the same configuration (*S* in Figure 1). The structure is closely related to that of $[L^1Zn_2(\mu\text{-OEt})Cl_2]$, reported by Williams et al.[9a] (Figure 2). However, for the chloride complex, the five-membered chelate rings have differing configurations (i.e., one ring is δ and the other λ), and this removes the rotational symmetry of the molecule. Although this configurational difference between the two structures may only be a solid-state packing effect (the chloride structure also contains a molecule of THF in the unit cell), it serves to highlight the flexibility of the ligand and the resulting complexity of the NMR spectra. The distance between the two zinc atoms in the chloride complex (3.176 Å) is similar to that in the iodide complex (3.1700(6) Å).

Although the ^{1}H NMR spectra and the X-ray crystal structures indicated formation of the desired ethoxide complexes, $[L^1Zn_2(\mu\text{-OEt})X_2]$, continued monitoring by ^{1}H NMR spectroscopy showed that these species were not stable in solution. Although the rate of change was slow at room temperature (several days to see formation of new peaks), at elevated temperatures the process occurred within several hours to give a mixture of products, including some of the starting trihalide species $[L^2Zn_2(\mu\text{-X})X_2]$ (particularly in the case of X = Cl). Nonetheless, the methathesis route to this type of bridging alkoxide dizinc complex is more straightforward and higher yielding than the alternative route described by Williams et al.[9a]

$[L^2Zn_2(\mu\text{-X})X_2]$. Because the NMe groups in the pendant arms in L^1 allow for the formation of various diastereoisomers, it was envisaged that removal of this group would simplify the NMR spectra of the resulting complexes. Thus, HL^2 (Scheme 1) was targeted for further study.

The halide complexes, $[L^2Zn_2(\mu\text{-X})X_2]$, were prepared in a similar manner to those of L^1 and were obtained in good yields (74−96%). The chloride and bromide complexes were both bright yellow solids, whereas the iodide complex was orange/yellow, and all three complexes had reduced solubility compared to the L^1 analogues. Unlike the complexes of L^1, all three halide complexes had very similar ^{1}H NMR spectra. In CD_2Cl_2, a single imine peak is observed at 8.38−8.40 ppm, and a single aromatic peak is found at ca. 7.26 ppm. The CH_2 groups are observed as broad peaks at 3.74−3.80 ppm and 2.86−2.94 ppm, although the latter peak is extremely broad. Two sharp singlets occur at 2.56−2.58 ppm and 2.24−2.32 ppm and are assigned to the NMe_2 groups and ArMe group, respectively. The ^{1}H NMR spectrum indicates that the complexes exist as a single symmetric species in solution, even in the case of the iodide complex. However, the broad nature of the CH_2 groups suggests that there may be significant fluxionality in the configuration of the *N*,*N*′ chelate rings. Indeed, low temperature ^{1}H NMR studies of $[L^2Zn_2(\mu\text{-I})I_2]$, in CD_2Cl_2, show that the broad signals associated with the CH_2 groups sharpen and split at 223 K, to give four multiplets at 4.02, 3.53, 3.18, and 2.60 ppm. In addition, the NMe_2 groups also split to give two sharp peaks, of 6H each, at 2.53 and 2.47 ppm, which is consistent with a chiral, symmetrical species.

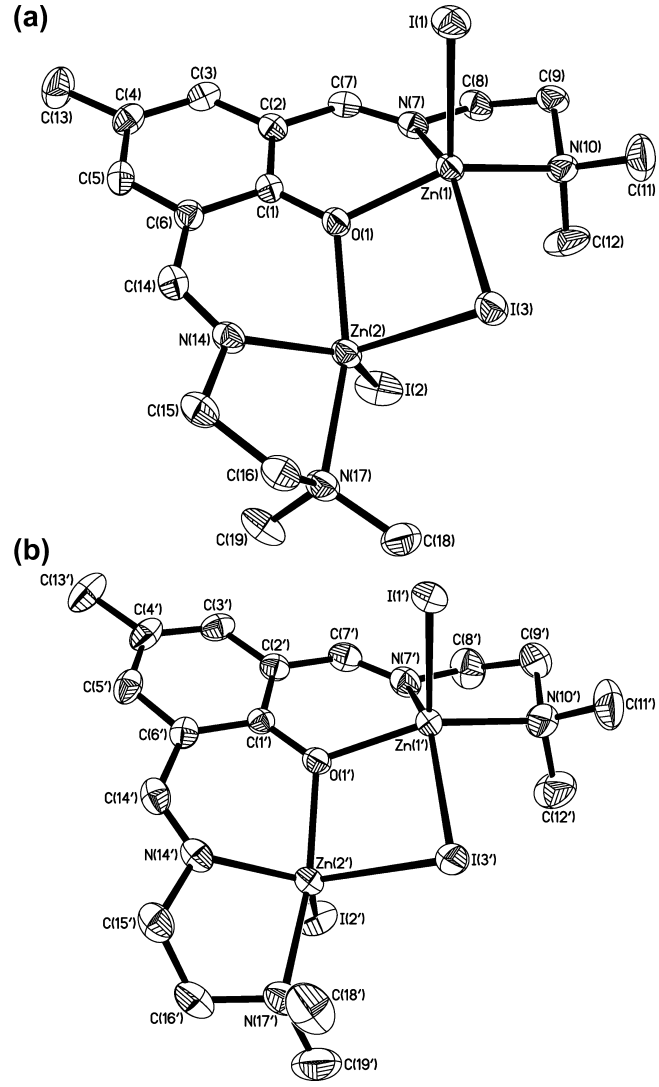

Figure 3. The molecular structures of (a) $[L^2Zn_2(\mu\text{-I})I_2]$-**I** and (b) $[L^2Zn_2(\mu\text{-I})I_2]$-**II**, the two crystallographically independent complexes present in the crystals of $[L^2Zn_2(\mu\text{-I})I_2]$ (both 50% probability ellipsoids).

X-ray Crystallography. The crystal structure of $[L^2Zn_2(\mu\text{-I})I_2]$ contains two independent complexes ($[L^2Zn_2(\mu\text{-I})I_2]$-**I** and $[L^2Zn_2(\mu\text{-I})I_2]$-**II**) with different configurations of the N(14)/N(17) *N*,*N*′ five membered chelate ring. In complex $[L^2Zn_2(\mu\text{-I})I_2]$-**I**, the chelate rings have opposite configurations (λ and δ respectively, Figure 3a), whereas in complex $[L^2Zn_2(\mu\text{-I})I_2]$-**II** the two rings have the same configuration (both λ, Figure 3b). (It is important to note that the complex crystallized in a racemic space group, so the crystal contains equal numbers of the complexes shown in Figure 3a and b, and their enantiomers). The isomer $[L^2Zn_2(\mu\text{-I})I_2]$-**I** is not observed in solution, as shown by the ^{1}H NMR spectra, which show a single symmetrical species, even at 193 K. As expected, in both independent complexes the C(7)—N(7) and C(14)—N(14) bonds lie much closer to the plane of the phenolate unit than was seen for their counterparts in the structure of $[L^1Zn_2(\mu\text{-OEt})I_2$, due to the constraints of the imine groups. The distances between the zinc centers (3.4248(5) and 3.4591(6) Å in complexes $[L^2Zn_2(\mu\text{-I})I_2]$-**I** and $[L^2Zn_2(\mu\text{-I})I_2]$-**II** respectively) are significantly longer than those observed for $[L^1Zn_2(\mu\text{-OEt})I_2]$. This effect prob-

ably relates to the improved donation from the imine versus amine groups, supported by the reduction in the length of the Zn—N(imine) bonds (between 2.059(3) and 2.086(3) Å) c.f. the Zn—N(amine) counterparts in $[L^1Zn_2(\mu\text{-OEt})I_2]$ (2.194(2) and 2.396(2) Å), and the associated ca. 9° widening of the Zn(1)—O(1)—Zn(2) angle.

$[L^2Zn_2(\mu\text{-OEt})X_2]$. In a similar manner to the L^1 complexes, the reactions of $[L^2Zn_2(\mu\text{-X})X_2]$ with potassium ethoxide were followed by ^{1}H NMR spectroscopy, using CD_3CN as the solvent and the compounds produced in quantitative yield. For $[L^2Zn_2(\mu\text{-Cl})Cl_2]$, a reaction occurred within an hour, and two new species were observed in the NMR spectrum, both of which were due to symmetrical products. The major species, ca. 85%, shows a new quartet at 3.97 ppm and a triplet at 1.36 ppm, assigned to a zinc-bound ethoxide group. The minor species also has zinc-ethoxide resonances at 3.53 and 1.11 ppm. The remaining peaks, that is, two new imine, aromatic, NMe_2, and $ArCH_3$ peaks, are all pairs of singlets in the ratio of 85:15. The CH_2 groups remain broad and overlap for the two species. The ^{1}H NMR spectra of the products of the reactions of $[L^2Zn_2(\mu\text{-Br})Br_2]$ and $[L^2Zn_2(\mu\text{-I})I_2]$ with potassium ethoxide were similar to those of $[L^2Zn_2(\mu\text{-Cl})Cl_2]$, although the ratios of the two symmetrical species were approximately 1:1 with the bromide complex and 3:7 with the iodide complex.

The precise structures of the two symmetrical alkoxide species remain unclear. The fluxionality of $[L^1Zn_2(\mu\text{-OEt})X_2]$ complexes has been noted, but the increased rigidity of L^2 is expected to increase the energetic barrier for interconversion of different conformations in the analogous complexes. If the $[L^2Zn_2(\mu\text{-OEt})X_2]$ complexes show related structures to L^1, then the two halide atoms could be on opposite sides of the plane of the molecule or on the same face. However, the X-ray crystal structures observed for this type of complex only show the halide groups on opposite sides of the plane of the molecule. Alternatively, different *N*,*N*′ chelate ring conformations could account for the two symmetrical species observed, although the barrier to conversion is expected to be significantly lower and is also likely to be the source of the broadening of the CH_2 peaks in the ^{1}H NMR spectra. In any event, a significant barrier to conversion exists since prolonged heating is required to cause changes in the relative ratios of the two species. Nevertheless, these complexes do not suffer from the decomposition or reformation of the trihalide species that were observed for the L^1 complexes.

$[L^3Zn_2(\mu\text{-X})X_2]$. The ligand flexibility was increased compared to L^1 and L^2 by synthesizing the related ligand, L^3 (Scheme 1). The zinc halide complexes, $[L^3Zn_2(\mu\text{-X})X_2]$, were synthesized by the same methods previously described and were white solids. The ^{1}H NMR spectra were similar to $[L^1Zn_2(\mu\text{-X})X_2]$; single peaks are observed for the aromatic, NMe_2, and the aromatic methyl protons, where X is chloride or bromide, and indicate that a single, symmetric species exists in solution, in each case. The peaks associated with the various differing CH_2 protons have increased multiplicity due to the presence of the NH protons. In the case of the iodide complex, and as with L^1, the ^{1}H NMR spectrum of $[L^3Zn_2(\mu\text{-I})I_2]$ is significantly broadened and shows evidence of various isomers. VT ^{1}H NMR (d_2-TCE) shows convergence of the peaks at 383 K, to give an averaged set of broadened signals.

$[L^3Zn_2(\mu\text{-OEt})Br_2]$. $[L^3Zn_2(\mu\text{-Br})Br_2]$ was treated with KOEt in a Youngs tap NMR tube, using CD_3CN as solvent. After 30 min the ^{1}H NMR spectra showed the complete disappearance of the starting material and the formation of several isomeric forms of $[L^3Zn_2(\mu\text{-OEt})Br_2]$. The spectrum is similar to those observed for $[L^1Zn_2(\mu\text{-OEt})X_2]$, although more peaks are observable in the aromatic region, which may be due to an increase in the number of isomers allowed by this less sterically hindered ligand. The integral of the aromatic region compared to the aliphatic and ethoxide regions is consistent with the formation of the desired species in quantitative yield.

$[L^{1-3}Zn_2(OAc)_3]$. The bimetallic zinc acetate complexes were prepared by treatment of the alkali salt of the ligands with $Zn(OAc)_2$. Using HL^1, a white solid was obtained. The ^{1}H NMR spectrum of this material is very broad, but shows a singlet at 6.76 ppm for the aromatic protons and a singlet at 2.18 ppm for the aromatic methyl group. There is a sharp singlet at 1.94 ppm that integrates to nine protons, and this has been assigned to the methyl protons for the three acetate groups. There are several very broad peaks between 2.55 and 4.40 ppm, which are attributed to the CH_2 protons and four broad peaks between 2.19 and 2.47 ppm, which have been assigned to the NMe groups. This compound was fluxional at room temperature, and the singlet observed for the acetate methyl protons suggests the differing acetate groups are in rapid exchange. VT-NMR spectroscopy showed that as the temperature was reduced some of the peaks began to sharpen, whereas others broadened and shifted. At 213 K, at least three peaks were seen in the aromatic region, and at least four peaks were observed for the acetate methyl groups. High temperature ^{1}H NMR studies (d_2-TCE) did simplify the spectrum, with coalescence of the peaks occurring to generate averaged resonances, although these peaks remained broad to 383 K. Nevertheless, elemental analysis and FAB mass spectrometry were in agreement with the structural formula of $[L^1Zn_2(OAc)_3]$.

Using L^2, gave a yellow/orange solid and simplified the analysis of the ^{1}H NMR spectrum. The peaks are all sharp, including the CH_2 groups that occur as two triplets at 3.70 and 2.80 ppm. This is in contrast to the halide complexes of L^2, where the CH_2 resonances are very broad in all cases. Sharp singlets are observed for the imine, aromatic, NMe_2, and ArMe protons, and only a single peak is observed for the three acetate methyl groups. The complex was symmetrical, and the single peak for the acetate groups indicates a rapid exchange process for this functional group. Reduced temperature ^{1}H NMR studies (CD_2Cl_2) did not alter the spectrum, apart from some broadening of the peaks, and only one acetate methyl group (integrating to nine protons) was observable down to 183 K.

The reaction of HL^3 with zinc acetate yielded a white solid. As with $[L^1Zn_2(OAc)_3]$, the ^{1}H NMR spectrum contained broad resonances. A singlet is observed for the aromatic protons, as well as the aromatic methyl group and the three

acetate groups. Two broad peaks are observed between 2.18 and 2.45 ppm, which integrate to 14 protons and are assigned to the NMe_2 groups and a CH_2 group. The series of at least seven broad peaks between 2.55 and 4.08 ppm are assigned to the remaining CH_2 and NH protons. Reduced-temperature ^{1}H NMR studies caused the peaks to sharpen, but several isomers were observed, although the acetate groups were differentiated at 193 K. High-temperature ^{1}H NMR studies showed coalescence of the peaks at 333 K to give a spectrum consistent with the formula $[L^3Zn_2(OAc)_3]$. Continued heating to 383 K caused a significant sharpening of the peaks.

In all three acetate complexes only a single peak for the acetate groups was observed in the ^{1}H NMR spectra, at room temperature. At least two different chemical environments are expected, depending on the number of bridging acetate units, but the NMR data indicates that the acetate groups are in rapid exchange around the zinc centers. Previously, zinc acetate complexes using this class of ligand have resulted in the formation of cationic species with a noncoordinating counterion (e.g., $[ClO_4]^-$, $[PF_6]^-$, or $[BF_4]^-$).[2g,h,k,4b,d−f,h,i,9d,10] Indeed, to our knowledge there is only one example of a complex containing two zinc centers and three coordinated acetate groups, only one of which is bridging.[4j] Therefore, it seems likely that the acetate complexes using L^{1-3} are cationic and contain two zinc centers bridged by two acetate groups. The third acetate group would be acting as a counterion (either weakly bound or noncoordinating), and is in rapid exchange with the coordinated acetate groups.

$[L^{1-3}Zn_2(\mu\text{-}OAc)_2][BPh_4]$. It was relevant to determine whether an acetate group could be exchanged with a noncoordinating counterion, and for these studies the tetraphenylborate anion was selected as it allows monitoring of the complexation by ^{1}H NMR spectroscopy. The complexes were readily synthesized by addition of sodium tetraphenylborate to a solution of HL^n and zinc acetate, in methanol, and the pure complexes were obtained in good yields (88−94%). The reaction using HL^1 yielded a white solid, and the ^{1}H NMR spectrum displayed very sharp peaks, which is in stark contrast to the spectrum of $[L^1Zn_2(OAc)_3]$. The tetraphenyl borate counterion signals are observed at 7.39, 7.01, and 6.87 ppm and integrate to 8, 8, and 4 protons, respectively. Single peaks are observed for the aromatic ligand protons, the NMe groups, the aromatic methyl group, as well as the acetate methyl protons, which integrate to six protons. Interestingly, the NMe_2 protons are observed as two singlets of six protons each, at 2.31 and 1.90 ppm. This ^{1}H NMR data indicates that the complex is chiral, symmetrical, and conformationally rigid.

The synthesis of $[L^2Zn_2(\mu\text{-}OAc)_2][BPh_4]$ yielded a yellow/orange solid. The ^{1}H NMR spectrum was also sharp and indicated that the expected complex was present. The NMe_2 groups, in this instance, were observed as a broad singlet, and this may be due to the increased rigidity of the ligand generating a planar structure. The reaction using HL^3 yielded a white solid and, as for the previous cationic complexes, the peaks in the ^{1}H NMR spectrum were sharp and in agreement with the formula $[L^3Zn_2(\mu\text{-}OAc)_2][BPh_4]$. The

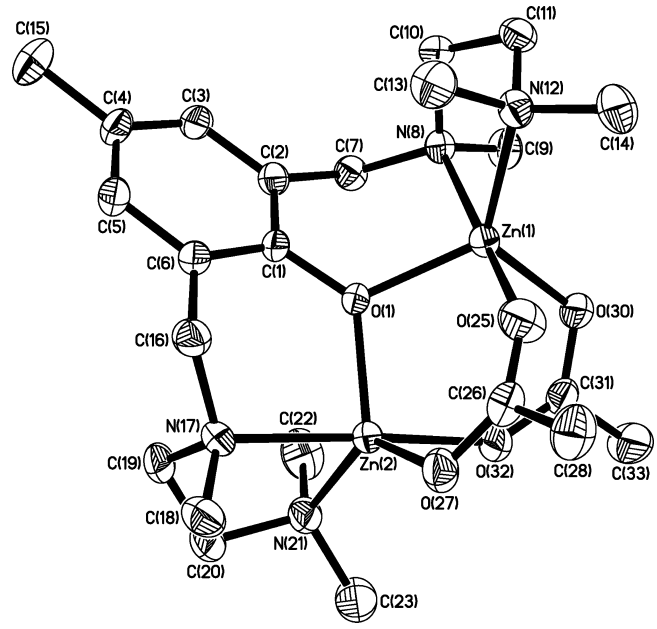

Figure 4. The molecular structure of $[L^1Zn_2(\mu\text{-}OAc)_2][BPh_4]$ (50% probability ellipsoids).

NMe_2 protons are observed as two singlets of six protons each, highlighting the chiral but conformationally stable nature of this complex.

X-ray Crystallography. The solid-state structures of $[L^{1-3}Zn_2(\mu\text{-}OAc)_2][BPh_4]$ show that the complex cations have approximate C_2 symmetry about an axis coincident with the C(1)—O(1) vector. In all the complexes, the two five-membered *N*,*N*′ chelate rings have the same chirality within each complex.[16] In Figure 4 both of the *N*,*N*′ chelate rings have λ twist geometries, whereas in Figures 5 and 6 the rings each have a δ twist geometry. However, as all the complexes crystallized in a centrosymmetric space group, there are equal numbers of the opposite enantiomers present in the crystals. As expected, the rigid imine groups in the complex of ligand L^2 (Figure 5) lie essentially coplanar with the phenolate ring. In the complexes of L^1 and L^3, however, the equivalent C—N single bonds are approximately orthogonal to this plane and on opposite sides, giving the complexes a chirality. It is notable that the specific enantiomers illustrated in Figures 4 and 6 have the same configuration for this chirality while having opposite chirality for the *N*,*N*′-five membered chelate rings (vide supra). It is also interesting to note, however, that the chirality at the amine nitrogens (N(8)/N(17) in $[L^1Zn_2(\mu\text{-}OAc)_2]^+$, and N(8)/N(16) in $[L^3Zn_2(\mu\text{-}OAc)_2]^+$), while the same within each complex, differ between the two ligands, being *S*,*S* in Figure 4 and *R*,*R* in Figure 6. Only one diastereoisomer of $[L^1Zn_2(OAc)_2][BPh_4]$ and $[L^3Zn_2(OAc)_2][BPh_4]$ are observed in the NMR spectra, thus highlighting

(16) In the structure of $[L^2Zn_2(\mu\text{-}OAc)_2][BPh_4]$, two orientations were found for the N(16)/N(19) five-membered chelate ring, one with the same configuration as the N(8)/N(11) chelate ring (ca. 66%) and one with the opposite configuration (ca. 34%). Complexes with the minor occupancy configuration of the N(16)/N(19) chelate ring clearly do not possess the approximate C_2 symmetry seen for complexes with the major occupancy configuration. The two configurations have slightly different positions for the N(19) donor atom, and only the major occupancy position has been considered in the discussion.

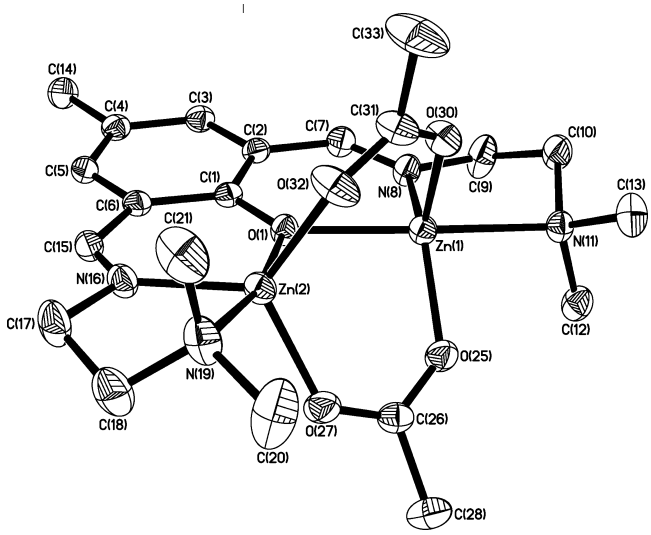

Figure 5. The molecular structure of $[L^2Zn_2(\mu\text{-}OAc)_2][BPh_4]$ (30% probability ellipsoids).

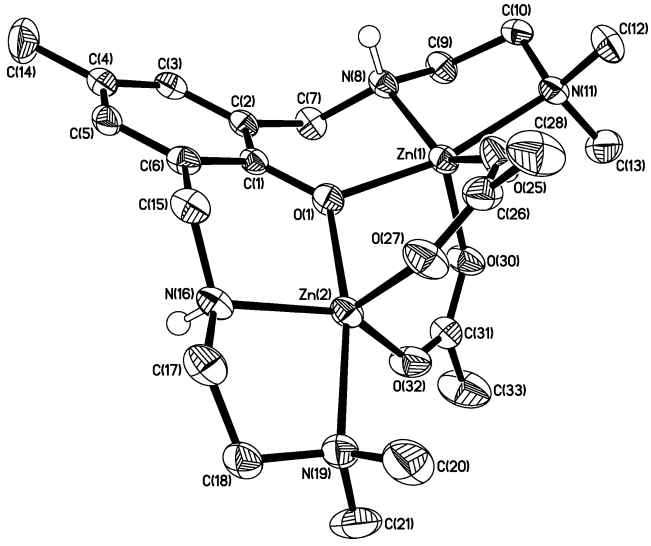

Figure 6. The molecular structure of $[L^3Zn_2(\mu\text{-}OAc)_2][BPh_4]$ (50% probability ellipsoids).

the coordinative flexibility of this system. The most obvious difference between the three complexes is the "gape" angle between the two acetate ligands, with the vectors from C(26) and C(31) subtending angles of ca. 93, 127, and 124° at the Zn(1)···Zn(2) centroid in complexes $[L^1Zn_2(\mu\text{-}OAc)_2][BPh_4]$, $[L^2Zn_2(\mu\text{-}OAc)_2][BPh_4]$, and $[L^3Zn_2(\mu\text{-}OAc)_2][BPh_4]$, respectively. Interestingly, this pattern extends to the metal···metal separation [3.1822(2), 3.2620(4), and 3.2580(5) Å in the complexes of L^1, L^2, and L^3, respectively]. The planar, rigid structure of coordinated L^2 results in the greatest intermetallic separation. The closer zinc−zinc distance in the case of L^1 versus L^3 is tentatively assigned to steric effects resulting from the methyl substituents.

Unlike the situation in the structures $[L^1Zn_2(\mu\text{-}OEt)I_2]$ and $[L^2Zn_2(\mu\text{-}I)I_2]$, the $[L^{1-3}Zn_2(\mu\text{-}OAc)_2][BPh_4]$ complexes have symmetric Zn−O(1) bonds (Tables 3−5), although they differ between the three complexes with those in $[L^2Zn_2(\mu\text{-}OAc)_2][BPh_4]$ (2.1035(13) and 2.1028(13) Å) longer than those in $[L^3Zn_2(\mu\text{-}OAc)_2][BPh_4]$ (2.035(2) and 2.031(2) Å),

Table 3. Selected Bond Lengths (Å) and Angles (°) for $[L^1Zn_2(\mu\text{-}OAc)_2][BPh_4]$

Zn(1)−O(1)	1.9666(10)
Zn(1)−N(8)	2.2176(13)
Zn(1)−O(25)	2.1538(12)
Zn(1)−O(30)	1.9670(11)
Zn(1)···Zn(2)	3.1822(2)
Zn(2)−O(1)	1.9669(10)
Zn(2)−N(17)	2.1868(13)
Zn(2)−O(27)	1.9626(11)
Zn(2)−O(32)	2.1435(11)
O(1)−C(1)	1.3535(17)
Zn(1)−O(1)−Zn(2)	107.99(5)

Table 4. Selected Bond Lengths (Å) and Angles (°) for $[L^2Zn_2(\mu\text{-}OAc)_2][BPh_4]$

Zn(1)−O(1)	2.1035(13)
Zn(1)−N(8)	2.0215(16)
Zn(1)−O(25)	1.9727(14)
Zn(1)−O(30)	1.9882(15)
Zn(1)···Zn(2)	3.2620(4)
Zn(2)−O(1)	2.1028(13)
Zn(2)−N(16)	2.0096(17)
Zn(2)−O(27)	1.9690(15)
Zn(2)−O(32)	1.9741(16)
O(1)−C(1)	1.315(2)
Zn(2)−O(1)−Zn(1)	101.70(6)

Table 5. Selected Bond Lengths (Å) and Angles (°) for $[L^3Zn_2(\mu\text{-}OAc)_2][BPh_4]$

Zn(1)−O(1)	2.035(2)
Zn(1)−N(8)	2.088(3)
Zn(1)−O(25)	1.978(3)
Zn(1)−O(30)	1.996(3)
Zn(1)···Zn(2)	3.2580(5)
Zn(2)−O(1)	2.031(2)
Zn(2)−N(16)	2.089(3)
Zn(2)−O(27)	1.987(3)
Zn(2)−O(32)	1.976(3)
O(1)−C(1)	1.342(4)
Zn(1)−O(1)−Zn(2)	106.51(11)

which are in turn longer than those in $[L^1Zn_2(\mu\text{-}OAc)_2][BPh_4]$ (1.9666(10) and 1.9669(10) Å). This is accompanied by a much longer Zn(1)−N(8) (2.2176(13) Å) distance in L^1, compared to the Zn(1)−N(8) (2.0215(16) Å) distance of L^2, and may be due to the increased constraint and coordinating strength of the imine units. The bond distances for the similar bonds of the L^3 complex are almost midway for those of L^1 and L^2. The angles around the zinc centers in the L^2 and L^3 complexes are very similar, whereas those for the L^1 complex are substantially different (see the Supporting Information), presumably due to the steric pressure from the N(8) and N(17) methyl groups.

Lactide Ring Opening Polymerization. Zinc alkoxide complexes have good precedent as initiators for the controlled polymerization of lactide.[12] In fact, zinc initiators have shown some of the fastest rates as well as excellent stereocontrol in lactide polymerization.[12] Previously, $[L^1Zn_2(\mu\text{-}OEt)Cl_2]$ was shown to be a rapid and controlled initiator,[9a] and the Mg(II) and Co(II) analogues were less effective.[9b] With the improved synthesis of $[L^nZn_2(\mu\text{-}OEt)X_2]$ complexes in hand, it was of interest to test the new complexes as initiators for lactide polymerization (Table 6).

The polymerizations were all conducted in methylene chloride at room temperature and at a loading initiator/lactide ratio of 1:200. The initiators were all generated in situ by reaction between the $[L^nZn_2(\mu\text{-}OEt)X_2]$ and KOEt, followed

Table 6. Polymerization of *rac*-Lactide[a]

complex	% conversion[b]	time/min	M_n[c]	PDI[c]
$[L^1Zn_2(\mu\text{-OEt})Cl_2]$	90	183	18 500	1.15
$[L^1Zn_2(\mu\text{-OEt})Br_2]$	91	22	18 500	1.15
$[L^1Zn_2(\mu\text{-OEt})I_2]$	98	1453	18 200	1.15
$[L^2Zn_2(\mu\text{-OEt})Br_2]$	91	4299	14 200	1.06
$[L^3Zn_2(\mu\text{-OEt})Br_2]$	92	1	23 800	1.06

[a] Polymerization conditions: $[LA]_0 = 1$ M, $[L^nZn_2(\mu\text{-OEt})X_2] = 5$ mM, CH_2Cl_2, 298 K. [b] Determined from the ^1H NMR spectrum by integration of the methylene resonances from polylactide (5.20 ppm) and lactide (5.00 ppm). [c] Determined from the SEC in THF using MALS detection to obtain the absolute molecular weights.

by removal of the KX byproduct and excess KOEt by filtration. Although an excess of KOEt was applied, the possibility of its interference on the polymerization can be discounted as KOEt has previously been shown to be a very poor initiator at room temperature.[12b] The polymerizations were compared by the time taken to reach a conversion of greater than 90%. A full kinetic study has already been undertaken with $[L^1Zn_2(\mu\text{-OEt})Cl_2]$ and established that it behaves in the usual manner, giving a second-order rate law with first-order dependencies on lactide and initiator concentration.[9a] Within the series of complexes using L^1, the relative order of rates is $[L^1Zn_2(\mu\text{-OEt})Br_2] > [L^1Zn_2(\mu\text{-OEt})Cl_2] > [L^1Zn_2(\mu\text{-OEt})I_2]$. The order does not correlate directly with the electronegativity of the halide element, with the bromide complexes showing the best rates. Thus, the bromide complexes of L^2 and L^3 were also tested: $[L^2Zn_2(\mu\text{-OEt})Br_2]$ was extremely slow, but $[L^3Zn_2(\mu\text{-OEt})Br_2]$ was very rapid, giving complete conversion in 1 min. The nature of the ancillary ligand has a significant influence on the rate: $L^3 \gg L^1 \gg L^2$; the slowest polymerization results from using the rigid, electron-rich imine ligand, whereas the fastest polymerization results from the flexible amine ligand. The polymerization control exerted by all initiators was reasonable; the polylactide produced had a narrow polydispersity index. The control over molecular weight was rather variable; the molecular weight expected for a 5 mM concentration of initiator and at >90% conversion is 26 000. The fit between experimental and theoretical molecular weight appears to correlate with the activity of the initiator, with the fastest initiator showing the best fit and the slowest initiator showing significantly lower molecular weights than the theoretical value. It is also notable that all the polymers show narrow polydispersity indices. A likely explanation for this behavior is that chain transfer is occurring; however, the source of the protic chain transfer agent (usually water or an alcohol group) is not currently clear. Chisholm has established that chain transfer occurs significantly more rapidly than propagation in lactide polymerization initiated by tin complexes.[17] It is clear that $[L^3Zn_2(\mu\text{-OEt})Br_2]$ holds the greatest potential for future development in terms of both its rate and polymerization control.

CO_2−Cyclohexene Oxide Copolymerisation. The copolymerisation of epoxides and CO_2 was first reported in 1969.[18] Recently, several more active and controlled catalysts have been developed, especially noteworthy are zinc phenoxide,[19] zinc β-diiminate,[14,20] and chromium(III) or cobalt(II) salen complexes.[21] The zinc β-diiminate complexes show very high turn-over frequencies (TOF), as well as excellent control.[13,18] Recent mechanistic studies, suggest that the most effective β-diiminate complexes are loosely associated dimers under the polymerization conditions. Coates and others have proposed that the two metal centers may be cooperating with one another, leading to enhanced rates. According to such a mechanism, one metal center activates the epoxide, which is subsequently attacked by a nucleophilic group bound to the other metal center, and this proposal has led to the deliberate preparation of various bimetallic zinc catalysts.[11c,f,h,22] The bimetallic complexes of this study were tested for copolymerisation activity, using cyclohexene oxide under 1 atm pressure of CO_2, at 50 °C for a period of 24 h. $[L^{1-3}Zn_2(\mu\text{-X})X_2]$ were activated with potassium ethoxide, PPN-Cl, and also DMAP, as previous studies using Cr(III) or Co(II) complexes have established that halide complexes and cocatalysts yield very active catalysts.[23] $[L^{1-3}Zn_2(\mu\text{-OAc})_3]$ and $[L^{1-3}Zn_2(\mu\text{-OAc})_2][BPh_4]$ were tested without addition of cocatalyst. In all cases, the new complexes failed to enable isolation of any significant quantity of polymer. Several of the complexes were also tested at higher pressures of CO_2 (7 bar) and higher temperature (80 °C), but again no activity was observed. The lack of catalytic activity may be due to the metal centers being sterically congested. The putative propagating species is a zinc carbonate, yet we have observed that this ligand system favors formation of cationic acetate complexes $[L^nZn_2(\mu\text{-OAc})_2]^+$.

Conclusions

We report the synthesis and characterization of a range of new bimetallic zinc complexes of the formula $[L^nZn_2(\mu\text{-X})X_2]$ (where X = Cl, Br, I, OEt, OAc), as well as the cationic acetate complexes, $[L^nZn_2(\mu\text{-OAc})_2][BPh_4]$. $[L^1Zn_2(\mu\text{-X})X_2]$ (where X = Cl, Br) showed NMR spectra consistent with a single symmetrical solution structure, but increasing the steric bulk of the X group to iodide and acetate groups led to multiple configurations in solution. The X-ray crystal

(17) Chisholm, M. H.; Delbridge, E. E.; Gallucci, J. C. *New J. Chem.* **2004**, *28*, 145.
(18) Inoue, S.; Koinuma, H.; Tsuruta, R. *J. Poly. Sci., Part B:Polym. Lett.* **1969**, *7*, 287.
(19) (a) Darensbourg, D. J.; Holtcamp, M. W.; Struck, G. E.; Zimmer, M. S.; Niezgoda, S. A.; Rainey, P.; Robertson, J. B.; Draper, J. D.; Reibenspies, J. H. *J. Am. Chem. Soc.* **1999**, *121*, 107. (b) Darensbourg, D. J.; Wildeson, J. R.; Yarbrough, J. C.; Reibenspies, J. H. *J. Am. Chem. Soc.* **2000**, *122*, 12487. (c) Darensbourg, D. J.; Zimmer, M. S.; Rainey, P.; Larkins, D. L. *Inorg. Chem.* **2000**, *39*, 1578.
(20) (a) Cheng, M.; Lobkovsky, E. B.; Coates, G. W. *J. Am. Chem. Soc.* **1998**, *120*, 11018. (b) Allen, S. D.; Moore, D. R.; Lobkovsky, E. B.; Coates, G. W. *J. Am. Chem. Soc.* **2002**, *124*, 14284. (c) Moore, D. R.; Cheng, M.; Lobkovsky, E. B.; Coates, G. W. *J. Am. Chem. Soc.* **2003**, *125*, 11911. (d) Eberhardt, R.; Allmendinger, M.; Luinstra, G. A.; Rieger, B. *Organometallics* **2003**, *22*, 211. (e) van Meerendonk, W. J.; Duchateau, R.; Koning, C. E.; Gruter, G. J. M. *Macromol. Rapid Commun.* **2004**, *25*, 382.
(21) (a) Paddock, R. L.; Nguyen, S. T. *J. Am. Chem. Soc.* **2001**, *123*, 11498. (b) Qin, Z. Q.; Thomas, C. M.; Lee, S.; Coates, G. W. *Angew. Chem., Int. Ed.* **2003**, *42*, 5484. (c) Darensbourg, D. J.; Yarbrough, J. C. *J. Am. Chem. Soc.* **2002**, *124*, 6335.
(22) (a) Xiao, Y. L.; Wang, Z.; Ding, K. L. *Chem. Eur. J.* **2005**, *11*, 3668. (b) Lee, B. Y.; Kwon, H. Y.; Lee, S. Y.; Na, S. J.; Han, S. I.; Yun, H. S.; LeeH.; Park, Y. W *J. Am. Chem. Soc.* **2005**, *127*, 3031.
(23) Darensbourg, D. J. *Chem. Rev.* **2007**, *107*, 2388.

structures show several potential sources of asymmetry, including the orientation of the $ArCH_2$ groups, the configuration of the N−R (R = Me or H) groups, as well as the ring configurations formed by the coordinated pendant arms. Further asymmetry may also arise from the configurations of the zinc centers themselves and, in particular, the positions of the X substituents. It is clear that complexes with L^1 and L^3 have flexible geometries,[24] whereas the imine unit in L^2 generates essentially planar complex geometries. Substituting the bridging halide group for an ethoxide group was achieved in quantitative yield using a salt metathesis reaction with potassium ethoxide. These alkoxide complexes were viable initiators for lactide ring opening polymerization, with the bromide complex using L^3 being extremely fast and well-controlled. The new complexes are not suitable catalysts for the copolymerization of carbon dioxide and epoxides, and this may be a result of steric crowding around the metal centers.

Experimental Section

Full experimental details for ligand and complex syntheses can be found in the Supporting Information; however, some examples of our standard complex syntheses are given here.

$[L^1Zn_2(\mu\text{-}Cl)Cl_2]$. In Air. A 25 mL round-bottomed flask with stir bar was charged with HL^1 (101 mg, 0.30 mmol), methanol (10 mL), and sodium methoxide (17 mg, 0.31 mmol). After the pale yellow/green solution was stirred for 15 min, zinc chloride (82 mg, 0.60 mmol) was added, and the solution rapidly decolorized. A white solid precipitated, and after stirring for a further hour, the mixture was filtered. The white solid was dissolved in dichloromethane and filtered through Celite. Removal of volatiles and drying under vacuum yielded a white solid (136 mg, 79%).

Under Dry Nitrogen. A Schlenk tube with stir bar was charged with HL^1 (200 mg, 0.59 mmol) and was placed under nitrogen. Dry THF (15 mL) was added, and the solution was cooled to −78 °C before transferring the solution to a Schlenk tube containing potassium hydride (35 mg, 0.89 mmol). A gas was evolved and the pale green solution turned yellow. The mixture was allowed to warm to room temperature and stirred overnight before filtering the solution into a Schlenk tube containing zinc chloride (162 mg, 1.19 mmol). The solution rapidly decolorized, and a large amount of white precipitate formed. Solvent was removed in vacuo, and the white solid was dissolved in dichloromethane, and then filtered. After removing the solvent and drying in vacuo, a white solid was obtained (275 mg, 81%). ^{1}H NMR (400 MHz, $CDCl_3$) δ ppm: 6.75 (s, 2H, Ar*H*), 4.36 (d, 2H, ArCH_2, $^2J_{HH}$ = 12 Hz), 3.11 (d, 2H, ArCH_2, $^2J_{HH}$ = 12 Hz), 2.86−3.00 (m, 4H, NCH_2), 2.61 (s, 12H, NMe_2), 2.54 (m, 2H, NCH_2), 2.45 (m, 2H, NCH_2), 2.16 (s, 9H, N*Me* and Ar*Me*). ^{13}C{^{1}H} NMR (100 MHz, $CDCl_3$) δ ppm: 158.3 (Ar), 131.8 (Ar*H*), 125.8 (Ar), 123.3 (Ar), 62.9 (ArCH_2), 56.2 (NCH_2), 55.8 (NCH_2), 47.2 (br, NMe_2), 43.8 (N*Me*), 20.1 (Ar*Me*). MS (FAB) *m/z* 572 $[M]^+$ (3%), 537 $[M-Cl]^+$ (56%), 464 (6%), 435 $[M-ZnCl_2]^+$ (9%), 376 (15%), 333 (72%). Elem. anal. found (calculated) for $C_{19}H_{35}Cl_3N_4OZn_2$ (%) C, 39.79 (39.85); H, 6.08 (6.16); N, 9.73 (9.78).

In Situ Generation of $[L^1Zn_2(\mu\text{-}OEt)Br_2]$. A Youngs tap NMR tube was charged with $[L^1Zn_2Br_3]$ (17.5 mg, 0.025 mmol) and potassium ethoxide (2.5 mg, 0.030 mmol). Deuterated acetonitrile was then added (ca. 0.5 mL), and the mixture was shaken. The resulting mixture was analyzed by ^{1}H NMR spectra after 30 min and showed formation of the title compound in quantitative yield. ^{1}H NMR (400 MHz, CD_3CN) δ ppm: 6.89−6.72 (m, 2H, Ar*H*), 4.30−2.99 (br m, 6 H, ArCH_2 and OCH_2CH$_3$), 2.90−2.00 (br m, 26 H, NCH_2, N*Me*, NMe_2, Ar*Me*), 1.49−1.02 (br m, 3H, OCH$_2$CH_3).

$[L^1Zn_2(OAc)_3]$. This complex has been synthesized in air and under nitrogen in a similar manner to the previous complexes, although the final product is soluble in most organic solvents, which can make purification difficult. Alternatively, a round-bottom flask was charged with HL^1 (228 mg, 0.68 mol), dichloromethane (2 mL), and hexane (10 mL). Sodium hydride [60% in mineral oil] (24 mg, 0.61 mmol) was then added, and the mixture was stirred for 2 h. After addition of zinc acetate (268 mg, 1.22 mmol), the mixture was stirred overnight, during which time a white precipitate formed that was filtered and dried (672 mg, 86%). Synthesis was also performed under dry nitrogen conditions. ^{1}H NMR (400 MHz, d_2-TCE, 303 K) δ ppm: 6.82 (s, 2H, Ar*H*), 4.33 (d, 2H, ArCH_2, $^2J_{HH}$ = 11 Hz), 3.13 (d, 2H, ArCH_2, $^2J_{HH}$ = 11 Hz), 2.93 (m, 4H, NCH_2), 2.62 (s, 12H, NMe_2), 2.50 (m, 4H, NCH_2), 2.23 (s, 3H, Ar*Me*), 2.16 (br s, 6H, N*Me*), 2.10 (s, 9H, O*Ac*). ^{13}C{^{1}H} NMR (100 MHz, d_2-TCE, 303 K) δ ppm: 176.9 (O*Ac*), 157.7 (Ar), 132.2 (Ar),127.3 (Ar), 123.4 (Ar), 61.7 (ArCH_2), 55.9 (NCH_2), 52.2 (br, NCH_2), 46.2 (NMe_2), 43.6 (N*Me*), 22.1 (O*Ac*), 20.2 (Ar*Me*). MS (FAB) *m/z* 583 $[M-OAc]^+$ (100%), 357 (14%). Elem. anal. found (calculated) for $C_{25}H_{44}N_4O_7Zn_2$ (%) C, 46.72 (46.67); H, 6.96 (6.89); N, 8.63 (8.71).

$[L^1Zn_2(\mu\text{-}OAc)_2][BPh_4]$. To a solution of HL^1 (55 mg, 0.16 mmol) in methanol (5 mL) was added $Zn(OAc)_2 \cdot 2H_2O$ (72 mg, 0.33 mmol). Upon stirring for several minutes, the zinc acetate fully dissolved, after which time sodium tetraphenylborate (59 mg, 0.17 mmol) was added. A white precipitate formed rapidly, and the mixture was stirred for 10 min. The white solid was filtered and dried (137 mg, 93%). Crystals suitable for X-ray crystallography were grown from ethanol. ^{1}H NMR (400 MHz, $CDCl_3$) δ ppm: 7.38 (br m, 8H, B−Ar*H*), 7.01 (t, 8H, B−Ar*H*, $^3J_{HH}$ = 7 Hz), 6.87 (t, 4H, B−Ar*H*, $^3J_{HH}$ = 7 Hz), 6.83 (s, 2H, Ar*H*), 3.92 (d, 2H, ArCH_2, $^2J_{HH}$ = 13 Hz), 3.11 (d, 2H, ArCH_2, $^2J_{HH}$ = 13 Hz), 2.69 (m, 2H, NCH_2), 2.56 (s, 6H, N*Me*), 2.55 (m, 2H, NCH_2), 2.31 (s, 6H. NMe_2), 2.24 (s, 3H, Ar*Me*), 2.09 (m, 2H, NCH_2), 2.02 (s, 6H, O*Ac*), 1.90 (s, 6H, NMe_2), 1.87 (m, 2H, NCH_2). ^{13}C{^{1}H} NMR (100 MHz, $CDCl_3$) δ ppm: 179.7 (O*Ac*), 164.3 (q, B−Ar, $^1J_{BC}$ = 49 Hz), 157.1 (Ar), 136.2 (B−Ar), 132.9 (Ar), 128.3 (Ar), 125.4 (B−Ar), 122.9 (Ar), 121.6 (B−Ar), 61.6 (ArCH_2), 55.9 (NCH_2), 49.6 (NCH_2), 48.6 (N*Me*), 44.0 (NMe_2), 43.6 (NMe_2), 23.5 (O*Ac*), 20.3 (Ar*Me*). MS (FAB) *m/z* 583 $[M-BPh_4]^+$ (77%), 357 (16%). Elem. anal. found (calculated) for $C_{47}H_{61}BN_4O_5Zn_2$ (%) C, 62.62 (62.47); H, 6.76 (6.80); N, 6.11 (6.20).

Acknowledgment. The EPSRC are acknowledged for funding the research (EP/C544846/1 and EPC544838/1). PURAC are thanked for the donation of *rac*-lactide.

Supporting Information Available: The full experimental section for all ligands and complexes prepared as well as details of the X-ray crystallography are available in the Supporting Information. This material is available free of charge via the Internet at http://pubs.acs.org.

IC8014173

(24) In a related system, α-methybenzyl groups were used as substituents on the inner nitrogen atom of the pendant arms in an attempt to control stereoselective substrate recognition for aminopeptidase models. Two preferable conformers were found by calculation from six possible conformers, assuming C_2 symmetry with a homochiral ligand. See ref 4I.